

Relationships between Leaf Area Index and Landsat TM Spectral Vegetation Indices across Three Temperate Zone Sites

David P. Turner,^{*} Warren B. Cohen,[†] Robert E. Kennedy,^{*}
Karin S. Fassnacht,[‡] and John M. Briggs[§]

*M*apping and monitoring of leaf area index (LAI) is important for spatially distributed modeling of vegetation productivity, evapotranspiration, and surface energy balance. Global LAI surfaces will be an early product of the MODIS Land Science Team, and the requirements for LAI validation at selected sites have prompted interest in accurate LAI mapping at a more local scale. While spectral vegetation indices (SVIs) derived from satellite remote sensing have been used to map LAI, vegetation type, and related optical properties, and effects of Sun–surface–sensor geometry, background reflectance, and atmospheric quality can limit the strength and generality of empirical LAI–SVI relationships. In the interest of a preliminary assessment of the variability in LAI–SVI relationships across vegetation types, we compared Landsat 5 Thematic Mapper imagery from three temperate zone sites with on-site LAI measurements. The sites differed widely in location, vegetation physiognomy (grass, shrubs, hardwood forest, and conifer forest), and topographic complexity. Comparisons were made using three different red and near-infrared-based SVIs (NDVI, SR, SAVI). Several derivations of the SVIs were examined, including those based on raw digital numbers (DN), radiance, top of the atmosphere reflectance, and atmospherically corrected reflectance. For one of the sites, which had extreme topographic complex-

ity, additional corrections were made for Sun–surface–sensor geometry. Across all sites, a strong general relationship was preserved, with SVIs increasing up to LAI values of 3 to 5. For all but the coniferous forest site, sensitivity of the SVIs was low at LAI values above 5. In coniferous forests, the SVIs decreased at the highest LAI values because of decreasing near-infrared reflectance associated with the complex canopy in these mature to old-growth stands. The cross-site LAI–SVI relationships based on atmospherically corrected imagery were stronger than those based on DN, radiance, or top of atmosphere reflectance. Topographic corrections at the conifer site altered the SVIs in some cases but had little effect on the LAI–SVI relationships. Significant effects of vegetation properties on SVIs, which were independent of LAI, were evident. The variability between and around the best fit LAI–SVI relationships for this dataset suggests that for local accuracy in development of LAI surfaces it will be desirable to stratify by land cover classes (e.g., physiognomic type and successional stage) and to vary the SVI. ©Elsevier Science Inc., 1999

INTRODUCTION

Leaf area index (LAI), or projected leaf area per unit ground surface area, is a key biophysical variable influencing land surface photosynthesis, transpiration, and energy balance (Running, 1990; Bonan, 1995). As LAI can be related to remotely sensed data, an LAI surface has been an important driver to some ecosystem productivity models applied at landscape to global scales (Running et al., 1989; Milner et al., 1996; Hunt et al., 1996; Martin and Aber, 1997), and in the biosphere–atmosphere interactions component of some general circulation models

^{*} Forest Science Department, Oregon State University, Corvallis

[†] USDA, Forest Service, Pacific Northwest Research Station, Forest Sciences Laboratory, Corvallis

[‡] Department of Forest Ecology and Management, University of Wisconsin, Madison

[§] Division of Biology, Kansas State University, Manhattan

Address correspondence to David P. Turner, Forest Science Department, Oregon State University, Corvallis, OR 97331. E-mail: turnerd@fsl.orst.edu

Received 25 April 1998; revised 15 April 1999.

(Chase et al., 1996). The NASA-sponsored Earth Observing System (EOS), more specifically the Moderate Resolution Imaging Spectroradiometer (MODIS) sensor, is intended to refine our ability to monitor land surface properties such as LAI, and the MODIS LAND Science Team (MODLAND) is charged with global mapping of LAI at a grain size of 1 km (Running et al., 1994).

The MODLAND LAI mapping approach will rely on MODIS imagery in conjunction with a canopy reflectance model (Myneni et al., 1997; Knyazikhin et al., 1999). This approach is based on the absence of a comprehensive database on LAI–reflectance relationships, and the requirement for an LAI estimation algorithm which is globally applicable. Validation of sensor data products is an important component of the EOS program, and one option in the case of MODIS LAI surfaces is inverting local, or generalized, empirical LAI–reflectance relationships. This article presents results from a step towards MODIS LAI validation, with a cross-site comparison of relationships between field-measured LAI and Landsat Thematic Mapper (TM) spectral vegetation indices (SVIs).

BACKGROUND

Early spectroradiometer measurements of visible and infrared energy identified a strong correlation between a red and near-infrared transmittance ratio and measured LAIs (Jordan, 1969). Because of high red energy absorption by chlorophyll, the principal light harvesting pigment in photosynthesis, plant foliage has relatively low transmittance (and reflectance) of red energy. In contrast, plant cell walls—notably the lignin component—cause scattering of near-infrared energy, resulting in relatively high near-infrared transmittance and reflectance (Gates et al., 1965). These observations suggested that a scanning sensor mounted on a boom, an airplane, or an Earth-orbiting satellite, might provide spectral measurements that are strongly related to the amount of leafy biomass or LAI (Tucker, 1979). The recognition that reflectance measurements offered the opportunity for “scaling up” from the plot level to larger areas has produced sustained interest over the last three decades in development of empirical algorithms relating LAI to surface reflectance and to spectral vegetation indices (SVIs) derived from reflectance.

Ratio-based indices are a subset of a diverse range of SVIs. Numerous ratio-based SVIs have been statistically related to LAI, with the most common being the simple ratio (SR) and the normalized difference vegetation index (NDVI) (Goward et al., 1991; Baret and Guyot, 1991; Huete et al., 1994; Price and Bausch, 1995; Teillet et al., 1997). Both of these are based on ratios of red (R) to near-infrared (NIR) reflectance: $SR = NIR/R$; $NDVI = (NIR - R)/(NIR + R)$. The appeal of R and NIR ratio-based indices is strongly rooted in the contrasting response of R

and NIR to increases in LAI from an unvegetated condition, and to a somewhat compensating effect on variations in reflectance caused by differences in Sun–surface–sensor geometry (Hall et al., 1995; Chen, 1996).

The alternative forms of band ratioing in SR and NDVI result in differential sensitivity to variations in R and NIR reflectance (Chen and Chilar, 1996). Under conditions of low LAI, where R is relatively high and NIR relatively low, a small change in R produces a larger proportional change in NDVI than SR. With higher LAI, for which NIR is generally higher and R lower, a change in NIR will induce a larger proportional change in SR than NDVI. The optimum SVI for a particular application may thus depend on the local LAI range.

Variation in background (soil and litter) reflectance can affect R–NIR SVIs. This has led to development of alternative formulations which include correction factors or constants introduced to account for, or minimize, the varying background reflectance (Huete, 1988; Huete and Tucker, 1991; Huete et al., 1994). In applications focused on overstory LAI, variability in reflectance from understory vegetation can likewise be problematical (Franklin, 1986; Spanner et al., 1990) and has inspired alternative SVIs incorporating mid-IR reflectance (Nemani et al., 1993). SVIs involving transformations based on band-specific coefficients have also been studied as a way of maximizing the information content of the index (Richardson and Wiegand, 1977; Jackson, 1983).

One general conclusion from the individual LAI–SVI studies is that there is considerable sensitivity to LAI, but more so at relatively low LAI values. Studies have included croplands (Wiegand et al., 1979; Asrar et al., 1984), grasslands (Friedl et al., 1994; Goetz, 1997), shrublands (Law and Waring, 1994), conifer forests (Running et al., 1986; Spanner et al., 1994; Chen and Chilar, 1996), broadleaf forests (Badwar et al., 1986; Fassnacht et al., 1997), and mixtures of vegetation types (White et al., 1997). R–NIR SVIs typically increase over an LAI range from 0 to about 3–5 before an asymptote is reached. The upper limit of sensitivity, and the relative importance of R and NIR reflectance in determining this limit, apparently differ among vegetation types.

Several factors potentially contribute to differences among vegetation types in their LAI–SVI relationships. At the leaf level, these include influences associated with variation in leaf pigments, leaf internal structure, and the orientation of the leaf relative to solar radiation (Baret and Guyot, 1991; Williams, 1991; Bouman, 1992; Yoder and Waring, 1994). Within tree crowns, variability is introduced by leaf clumping of various types which causes shading at a fine spatial scale, and the contribution of woody material to total reflectance (Guyot et al., 1989; Williams, 1991; Huemmrich and Goward, 1997). At the multitree scale, heterogeneity in tree height and the number and size of tree gaps influences reflectance

Table 1. Summary of Site-Level Information

Site	Vegetation Types	Number of Plots	LAI Measurement Method	LAI Range	TM Scene Date
KNZ	Burned grassland	6	Clipping	2.5–6.3	15 August 1993
	Unburned grassland	7	Clipping	2.5–3.2	
NTL	Broadleaf forest	14	Litterfall	4.4–8.4	10 August 1993
	Conifer forest—young	10	Litterfall	1.4–3.9	
AND	Shrubland	3	Plant cover	1.0–3.3	9 August 1994
	Conifer forest—young	6	Sapwood area	5.3–9.6	
	Conifer forest—old	7	Sapwood area	7.9–13.0	

(Guyot et al., 1989; Cohen et al., 1990; Cohen and Spies, 1992; Leblon et al., 1996).

Additional factors potentially altering SVIs independently of LAI concern Sun–surface–sensor geometry and atmospheric scattering and absorption of radiation (Meyer et al., 1993; 1995; Myneni and Asrar, 1994; Deering et al., 1994; Chen and Cihlar, 1996). Several methods to compensate for these exogenous effects have been attempted (e.g., Spanner et al., 1990; 1994). However, results are commonly mixed and there have been few tests of their influence on LAI–SVI relationships.

The objective of this study was to examine the generality of empirical TM-based LAI–SVI relationships across a variety of vegetation types and a wide range of LAIs. Earlier studies have often treated only one vegetation type, and comparisons across studies have been hampered by variations in sensor characteristics and by variations in image processing methods. The emphasis here was on evaluating the LAI–SVI relationships across a variety of vegetation types with an attempt to control exogenous factors.

METHODS

The study involved three National Science Foundation Long Term Ecological Research sites (Table 1) differing widely in vegetation physiognomy, climate, and topography. Vegetation types at the three sites included grassland, shrubland, hardwood forest, and conifer forest. LAI, defined here as the projected leaf area per unit ground surface area ($\text{m}^2 \text{m}^{-2}$) ranged from 1 to 13, nearly the range of LAI represented across all of North America (Cannell, 1982). Slope was generally minimal except at the H. J. Andrews site which has considerable topographic complexity. At each site, measurements of LAI were made at a number of plots with locations determined by the Global Positioning System (GPS). The LAI measurements were made independently at each site. Relationships of LAI to three ratio-based spectral vegetation indices (SVIs) derived from TM imagery were examined.

LAI Measurements

Konza Prairie Research Natural Area (KNZ)

The KNZ site is in the tallgrass prairie region of east central Kansas (Van Cleve and Martin, 1991; Briggs and Knapp, 1995). This landscape is subject to controlled burning and grazing. The LAI measurements for this study were all on grassland-dominated plots which were located in an area protected from grazing but in some cases burned at the beginning of each growing season. Thirteen plots were used in the study, six burned (annually for >15 years) and seven unburned (for >10 years), with each plot representing a small watershed. Unburned plots have a significant carryover of dead material from growth in previous years. Biomass measurement protocols for the plots are described elsewhere (Briggs and Knapp, 1995; Su et al., 1996). Briefly, at each plot a total of 20 quadrats (each 0.1 m^2) were harvested (clipped) along a 100–200 m transect. Samples were sorted into live graminoid, live forb, and dead material. Clipping was done in 1993 at the time of maximum live biomass (early August), close to the time of image acquisition. In 1996, specific leaf areas ($\text{cm}^2 \text{g}^{-1}$) at the same study site were determined for graminoids and forbs from leaf area measurements made with a CID Laser (CID Inc., Vancouver, WA) leaf area meter. LAIs in 1993 were then estimated from the 1993 biomass values.

North Temperate Lakes (NTL)

Data for the NTL site in North Central Wisconsin represented second growth, mixed conifer–hardwood forest (Van Cleve and Martin, 1991). The study area and LAI measurement procedures are described more fully in Fassnacht et al. (1997). Twenty-four stands were sampled, four each from six of the major habitat types in the area. Stands were chosen to be representative of the species composition and range of LAIs in the upland forests of that region. For this study, each stand was classified as young conifer (<75 years) or broadleaf-dominated, depending on the major contributor to overstory LAI. LAI was estimated for each stand from litterfall, specific leaf area (SLA), and leaf turnover time. Litterfall was collected periodically from Summer 1992 to Spring 1994 in ten $1 \text{ m} \times 1 \text{ m}$ litter screens for each stand. Leaf litter

was sorted by species, and SLA was determined with a Delta-T Image Analyzer (Decagon Devices, Pullman, WA) for conifer species and an LAI-3000 (Li-Cor, Inc., Lincoln, NE) for broadleaf species. Species-specific leaf turnover times were derived from the literature (Barnes and Wagner, 1981).

H. J. Andrews Experimental Forest (AND)

The AND site is on the west slope of the Oregon Cascade Range and is predominately temperate coniferous forest (Van Cleve and Martin, 1991). Sixteen stands in or near the Andrews Experimental Forest were sampled in summer of 1997 for this study, including clearcut areas dominated by herbs and shrubs, young (<80 years) closed-canopy conifer plantations, and mature to old-growth native coniferous forests (Means et al., 1999). In each stand a 50 m × 50 m plot, with dimensions corrected for slope angle, was sampled.

For the herb- and shrub-dominated plots, percent cover for each herbaceous species (ocular estimate) and stem diameters for all shrubs were measured in five circular subplots (78 m²) per stand. The summed percent herbaceous cover was divided by 100 to estimate herbaceous LAI. This approach may yield a underestimate of LAI when there is extensive intraspecific overlap of foliage, but this was generally not the case in this study. For shrubs, stem diameters were converted to foliar biomass using the allometric relationships of Means et al. (1994) and shrub LAIs were estimated using an average specific leaf area of 250 cm² g⁻¹ (Waring et al., 1977). For tree-dominated stands (cover >85%), canopy LAI was estimated from sapwood cross-sectional areas and species-specific sapwood area to leaf area ratios. Sapwood areas were estimated from tree diameter at breast height (DBH) distributions which were determined in 5–25 subplots, depending on tree size. All trees with height greater than 1.37 m were identified by species and measured for DBH to the nearest centimeter. The species-specific parametrizations relating DBH to sapwood area and sapwood area to leaf area were from Zelig-PNW, a forest gap model which has been developed for applications in Pacific Northwest conifer forests (Urban, 1993; Urban et al., 1993; Hansen et al., 1993). Because of potential errors associated with most all approaches to estimating LAI in old-growth conifer stands (Turner et al., 1999), the estimates for those stands remain the most uncertain.

Image Processing

A single TM image was obtained for each site (Table 1). The AND and KNZ scenes were purchased unrectified but were registered to existing georectified images using nearest neighbor resampling. Image to image root mean squared error for the study area was 25 m using 170 Ground Control Points (GCPs) at AND and 18 m using 16 GCPs at KNZ. The TM scene for NTL was pur-

chased as a precision georectified product (Fassnacht et al., 1997). For all images, digital numbers (DNs) were converted to radiance (RAD) and top-of-atmosphere reflectance (ρ_{TOA}) according to the procedures outlined in Markham and Barker (1986). Sensor gain, sensor bias, sun elevation, and Sun azimuth values were obtained directly from image headers. Surface reflectance (ρ_{SUR}) was calculated using the 6S software developed at Goddard Space Flight Center (Quadrari and Vermote, 1999, this issue).

Because AND has enough topographic variation to potentially affect the relationship between LAI and the SVIs, three topographic corrections were applied to the ρ_{SUR} image of AND. The methods for the three corrections used here are summarized in Meyer et al. (1993) and include: 1) the cosine correction (COS), 2) the statistical-empirical additive correction (ADD) and 3) the C- or multiplicative correction (MULT). The correction factor for the first method is simply a ratio between the cosine of the incidence angle and the cosine of the Sun's zenith angle for a given pixel, and is the same for all image bands. The latter two approaches fit a regression line to the relationship between pixel value and the cosine of incidence angle and mathematically remove any trends using either an additive (statistical-empirical approach) or a multiplicative adjustment (C-correction). A different correction factor was determined for each image band. Elevation data was obtained from standard 7.5-min USGS digital elevation models (Level II) with 30-m pixel size.

For each of the 53 plots across all sites, a mean value was derived for each image variable. The average for a 3 × 3 pixel window surrounding the plot center was used in the case of AND and NTL. At KNZ, the average for 9–14 TM pixels associated with the 20 quadrats was employed. The coefficient of variation in these windows was generally less than 10%. For all three sites, the date of image acquisition approximated the time of maximum foliar biomass.

LAI-SVI Relationships

The SVIs used in the study were the NDVI, the SR, and the soil adjusted vegetation index (SAVI) (Huete et al., 1997). Formulations for the NDVI and SR were given earlier. The calculation of SAVI is as follows [Eq. (1)]:

$$SAVI = (1 + L) * (NIR\rho_{SUR} - R\rho_{SUR}) / (NIR\rho_{SUR} + R\rho_{SUR} + L) \quad (1)$$

with L equal to 0.5 in this study. Several variants of each SVI were derived from the image data (Table 2). For each site, the NDVI was derived from DN (NDVI_{DN}), radiance (NDVI_{RAD}), top of atmosphere reflectance (NDVI_{TOA}), and surface reflectance (NDVI_{SUR}). This was done to test the effects of spectral data processing level on the strength of the relationships between NDVI and LAI. A similar procedure was followed with SR and, except for omission of the DN and RAD versions, with SAVI. As the results of this step indicated the superiority of surface reflectance

Table 2. Summary of SVI Images Prepared by Site and Stage of Image Processing

Site	Digital Number	Radiance	Stage of Image Processing		Topographic Correction		
			TOA Reflectance	Surface Reflectance	COS	ADD	MULT
AND	NDVI	NDVI	NDVI	NDVI	NDVI	NDVI	NDVI
	SR	SR	SR	SR	SR	SR	SR
	—	—	SAVI	SAVI	SAVI	SAVI	SAVI
KNZ	NDVI	NDVI	NDVI	NDVI	—	—	—
	SR	SR	SR	SR	—	—	—
	—	—	SAVI	SAVI	—	—	—
NTL	NDVI	NDVI	NDVI	NDVI	—	—	—
	SR	SR	SR	SR	—	—	—
	—	—	SAVI	SAVI	—	—	—

derived SVIs ($NDVI_{SUR}$, SR_{SUR} , and $SAVI_{SUR}$), we then focused on relationships between LAI and these forms across sites. To test the effects of topographic corrections at AND, the three SVIs were further derived from each of the three topographic corrections applied to the AND reflectance data: cosine ($NDVI_{COS}$, SR_{COS} , and $SAVI_{COS}$), additive ($NDVI_{ADD}$, SR_{ADD} , and $SAVI_{ADD}$), and multiplicative ($NDVI_{MULT}$, SR_{MULT} , and $SAVI_{MULT}$).

Least squares regression analysis (SAS Institute Inc., 1990) with LAI as the independent variable was used to evaluate the relationships between LAI and each of the SVIs. The models investigated were linear, logarithmic, quadratic polynomial, and cubic polynomial. The polynomial models were added after preliminary results indicated a modest decrease in the SVIs at the highest LAIs. The results are reported in terms of the adjusted R^2 and, in order to account for varying ranges in the SVIs, the quotient of the standard error of the y estimate (SEE) and the mean of the y values (\bar{Y}). To evaluate the relative influence of red and near-infrared reflectance on the LAI–SVI relationships, plots of LAI against $R\rho_{SUR}$ and $NIR\rho_{SUR}$ were also inspected.

The effects of the three topographic corrections on $NDVI_{SUR}$, SR_{SUR} , and $SAVI_{SUR}$ were investigated at the AND site by comparing values before and after correction. Similar comparisons for $R\rho_{SUR}$ and $NIR\rho_{SUR}$ provided insight into the differential effects of the corrections on the SVIs.

RESULTS

LAI Estimates

The range of LAIs across all sites was from 1.0 to 13.0 $m^2 m^{-2}$ (Table 1). Among the nonforested plots, the clearcut areas at AND had the lowest LAIs. The unburned grassland plots at KNZ were next highest and were all clustered around an LAI of about 3. The burned grassland plots at KNZ had higher LAIs and a broader LAI range. The year 1993 was one of the wettest years on record (Briggs and Knapp, 1995) with correspond-

ingly high productivity and LAI. For broadleaf-dominated plots, the LAI range was 4.4–8.4, with the highest LAI values near the maximum reported for this vegetation type (Burton et al., 1991). For conifer-dominated plots, the lowest LAIs were found in the stands on glacial outwash at NTL, intermediate LAIs were found in young stands at AND, and the highest values were in the older forests at the AND site.

Effects of SVI Derivation on

LAI–SVI Relationships

SVI derivation affected the shapes and strength of the LAI–SVI relationships. Trends were similar across the SVIs. Results for NDVI are presented as a case study (Table 3, Fig. 1). For all derivations, a cubic polynomial model gave a better fit (R^2) for the LAI–NDVI relationship than did linear, logarithmic or quadratic polynomial models. The cubic term was significant ($p < 0.05$, sum of squares F-test) in each case. In all derivations, the peak was reached between LAIs of 4–6, and there was a general decline in the NDVI at the highest LAIs. The R^2 for $NDVI_{SUR}$ was notably higher than those of the other derivations.

Similarities and Differences among the SVIs

A similar general pattern in the relationship of LAI to the surface-reflectance-derived SVI (SVI_{SUR}) was observed for all the SVIs (Figs. 1d, 2a, 2b). The SVI_{SUR} initially increased at low LAIs, peaked at intermediate values, and decreased at the highest LAIs. The quadratic polynomial gave a better fit than the cubic polynomial in the case of SR_{SUR} and $SAVI_{SUR}$ because there was more variability in the high LAI plots than was the case for $NDVI_{SUR}$. The adjusted R^2 and SEE/\bar{Y} were similar for SR_{SUR} and $SAVI_{SUR}$ but R^2 was appreciably higher and SEE/\bar{Y} appreciably lower for $NDVI_{SUR}$ (Table 3).

The variation in $NIR\rho_{SUR}$ was the dominant factor contributing to the changes in SVIs over the whole range of LAIs. The dynamic range for $NIR\rho_{SUR}$ across all plots was from 15% to 37% (Fig. 3) with generally increasing

Table 3. The Best Fit Model, Adjusted R^2 and SEE/\bar{Y} for the LAI-NDVI Relationship using Four Derivations of NDVI, and for the LAI- SR_{SUR} and LAI- $SAVI_{SUR}$ Relationships

Y	Model	R^2	SEE/\bar{Y}
$NDVI_{DN}$	$0.2926+0.1528x-0.0189x^2+0.0007x^3$	0.53	0.09
$NDVI_{RAD}$	$0.3195+0.1405x-0.0166x^2+0.0006x^3$	0.51	0.10
$NDVI_{TOA}$	$0.4939+0.1091x-0.0130x^2+0.0004x^3$	0.51	0.06
$NDVI_{SUR}$	$0.5724+0.0989x-0.0114x^2+0.0004x^3$	0.74	0.04
SR_{SUR}	$2.2282+2.5376x-0.1576x^2$	0.59	0.19
$SAVI_{SUR}$	$0.2318+0.0703x-0.0041x^2$	0.54	0.14

values as LAI increased except for the older conifer stands. The range for $R\rho_{SUR}$ was from 1.5% to 6% with all but two plots below 3% and little trend over the range of LAIs. The greater variability in SR_{SUR} and $SAVI_{SUR}$ compared to $NDVI_{SUR}$ relates to their greater dependence on $NIR\rho_{SUR}$.

With respect to patterns within vegetation types (Figs. 1d, 2), the shrub plots at AND had relatively low LAIs and low SVI_{SUR} . Over the narrow LAI range of the unburned grassland plots, none of the indices exhibited much variation, nor did they vary much over the large LAI range of the burned grassland plots. The broadleaf plots similarly all had essentially the same $NDVI_{SUR}$ but did vary considerably in SR_{SUR} and $SAVI_{SUR}$. The indices increased with LAI in young conifer stands in each case, but the relationship differed in that $NDVI_{SUR}$ was asymptotic at an LAI of about 5, the SR_{SUR} was highly variable above an LAI of 4, and $SAVI_{SUR}$ had a strong linear relationship over the whole LAI range ($R^2=0.94$). Within the set of old conifer plots at AND, SVI_{SUR} was generally lower than in the set of young conifer plots at AND, and there was no trend within the group with increasing LAI.

Effects of Topographic Corrections

The three corrections for topographic effects at AND altered the red and near-infrared reflectance to varying degrees (Fig. 4). Results for the MULT and ADD corrections were virtually the same and smaller than the effects of the COS correction. The lowest reflectance values were increased by a factor of over 2 in some cases.

Because the same correction is applied to all bands, the COS correction had no effect on the $NDVI_{SUR}$ and SR_{SUR} (Fig. 5). Large effects were evident in the case of SAVI with changes from -10% to +50% of the uncorrected values. There was not, however, an appreciable tightening of the LAI- $SAVI_{SUR}$ relationship. The linearity ($R^2=0.91$) of the LAI- $SAVI_{SUR}$ relationship for the set of young conifer and shrub plots (excluding the anomalous older stands) was largely lost after the COS correction ($R^2=0.56$). The ADD and MULT corrections are band-dependent and consequently did alter the SVI_{SUR} in each case. The changes were small for $NDVI_{SUR}$ and SR_{SUR} but as much as 20% for some of the $SAVI_{SUR}$ values. As with

the COS correction, there was no improvement in the LAI- $SAVI_{SUR}$ relationship.

DISCUSSION

Effects of Image Processing

The significant changes in the SVI values observed at different stages of image processing suggest the importance of converting to ρ_{SUR} whenever SVIs are compared across sites (see also Goward et al., 1991). The difference between NDVI expressed as DN and expressed as radiance is small because the calibration coefficients for TM 3 and TM 4 are similar (Markham and Barker, 1986). When $NDVI_{TOA}$ is compared with $NDVI_{RAD}$, differences can be expected because the solar constant for NIR is smaller than for R (Markham and Barker, 1986). The difference between the $NDVI_{RAD}$ and $NDVI_{TOA}$ would also depend on the difference in the solar zenith angles if comparisons were made across sites. In deriving $NDVI_{SUR}$, an increase has been applied to NIR primarily to correct for water vapor absorption (Justice et al., 1991; Goetz, 1997), but a decrease has been applied to R to remove the effect of scattering by the atmosphere. Thus, significant differences between $NDVI_{TOA}$ and $NDVI_{SUR}$ could be expected depending on elevation, atmospheric humidity, and haziness.

The improvement in adjusted R^2 for the LAI-NDVI relationship across sites when using ρ_{SUR} compared to DN, radiance, or ρ_{TOA} , indicates that the image processing tends to reduce rather than increase noise in the relationship. This improvement would be expected since the three Landsat TM scenes were different in terms of Sun-surface-sensor geometry as well as optical properties of the atmosphere. Other cross-site studies of LAI and remotely sensed SVIs have likewise found a better fit in LAI-SVI relationships after atmospheric correction of TOA reflectance data (Peterson et al., 1987; Spanner et al., 1990).

The benefits of the additional corrections for topographic effects are less evident. Visual inspection of single band images for the AND site after the COS, MULT, and ADD corrections for topographic effects revealed significant improvements in terms of removing patterns in reflectance associated with aspect. On single

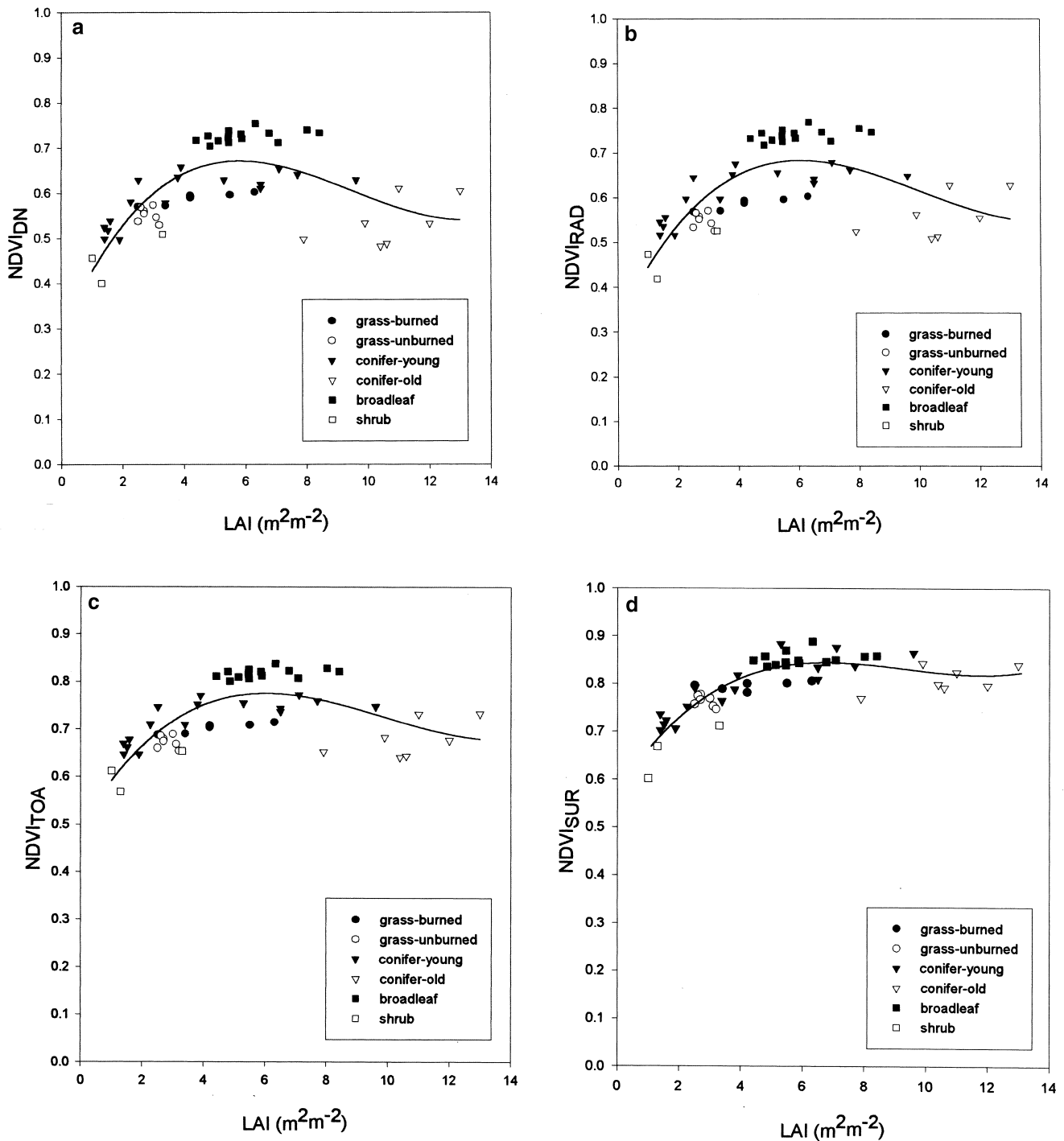


Figure 1. Effects of different stages of image processing on the LAI–NDVI relationship across all sites: a) digital number, b) radiance, c) top of atmosphere reflectance, d) surface reflectance. Lines are least squares fit to a cubic polynomial model. See Table 3 for the model and adjusted R^2 in each case.

band plots (not shown) of LAI vs. topographically corrected surface reflectance, the R and NIR reflectance for the three shrub-dominated plots were brought into much closer agreement. As noted, the COS correction does not influence the ratio-based SVIs but the empirical corrections (MULT, ADD) could be expected to affect the SVIs, and perhaps improve the fit for the LAI–SVI rela-

tionship. These corrections were large in some cases, but there was no apparent improvement in the fit for the LAI–SVI relationships as a result of the corrections.

Differences among the SVIs

Earlier studies have documented differential sensitivity to surface biophysical properties among the SVIs (Epi-

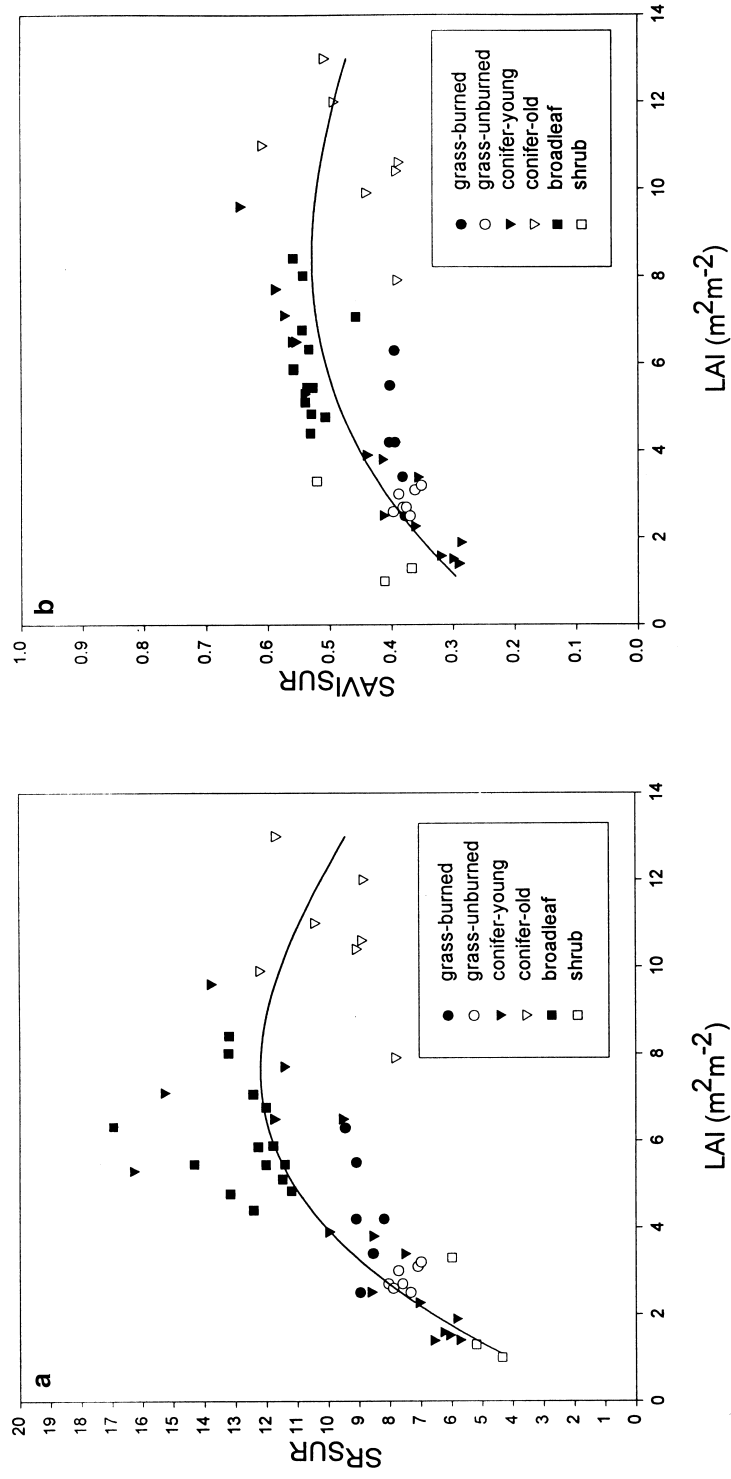


Figure 2. LAI-SVI relationships across all sites: a) SR, b) SAVI. See Figure 1d for NDVI. Lines are least squares fit to a quadratic polynomial model. See Table 3 for the model and adjusted R^2 in each case.

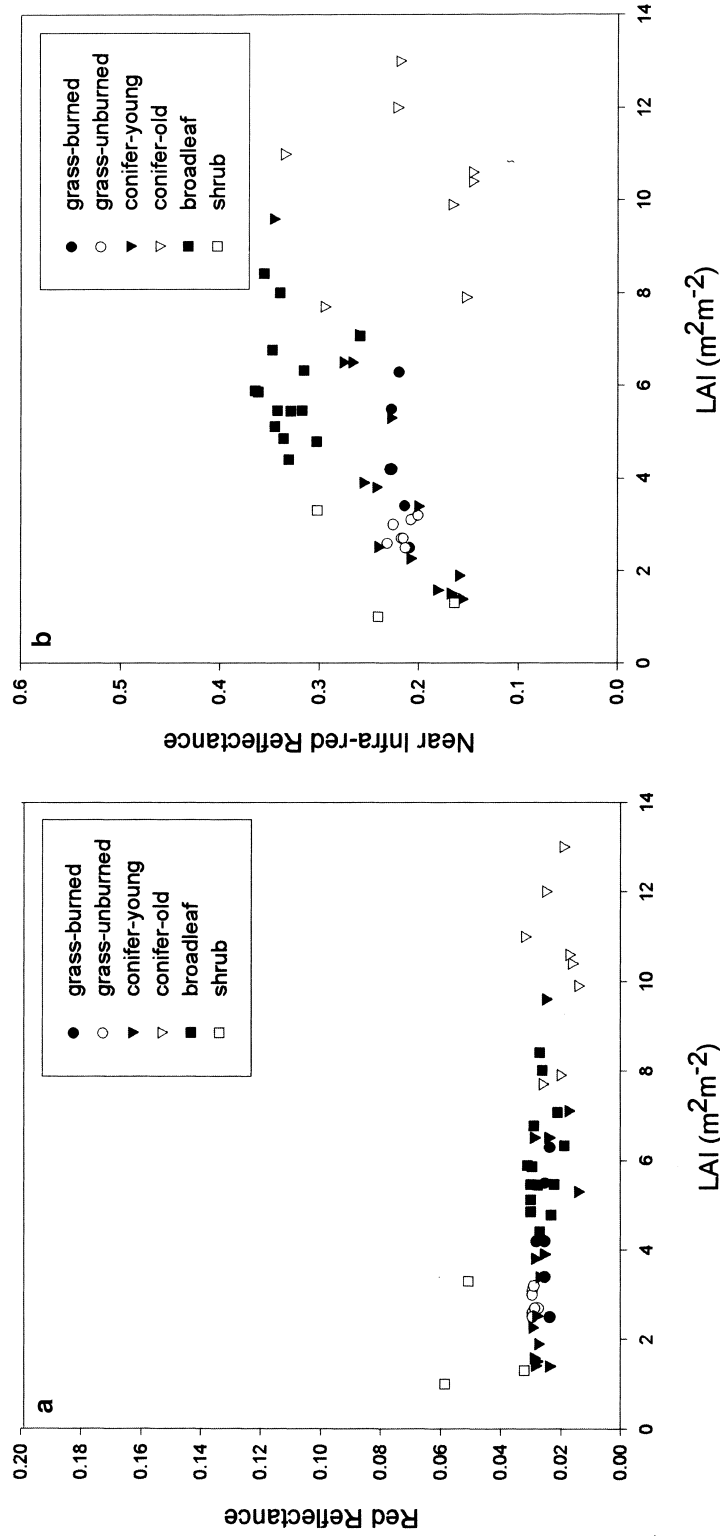


Figure 3. Relationship across all points for LAI and surface reflectance: a) red (TM 3), b) near-infrared (TM 4).

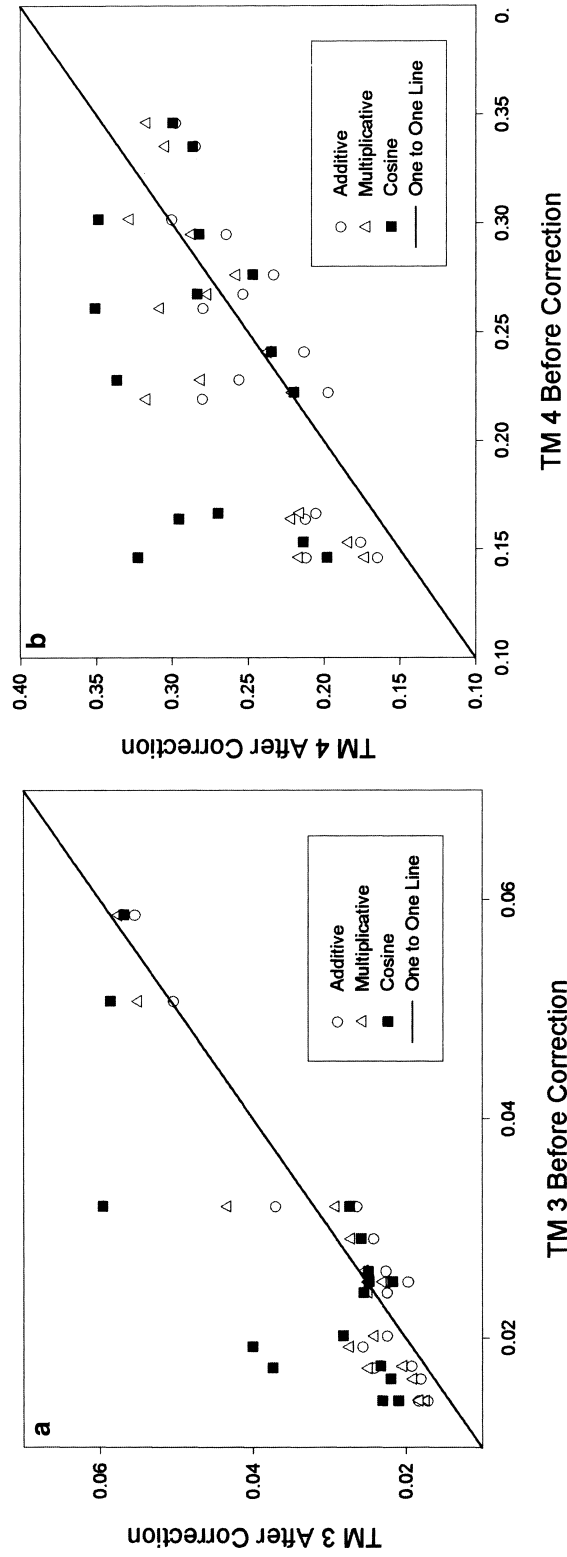


Figure 4. Effects of the topographic corrections at AND on surface reflectance: a) red (TM 3), b) near-infrared (TM 4).

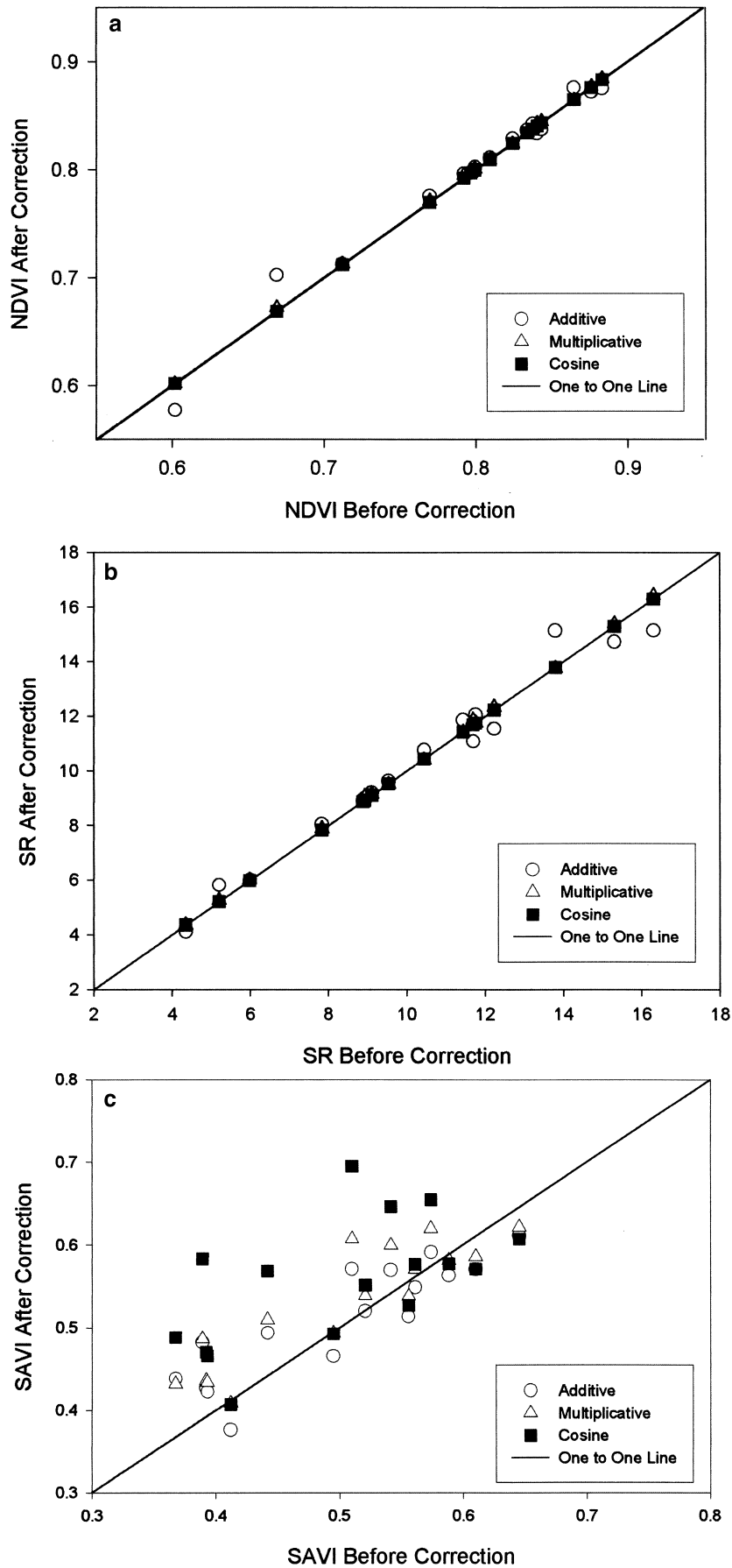


Figure 5. Effects of the topographic corrections at AND on the a) NDVI , b) SR, and c) SAVI.

phanio and Huete, 1995; Chen and Cihlar, 1996, White et al., 1997). For the observations in this study, increases in NIR reflectance with increasing LAI were more prominent than were decreases in R reflectance. Thus the SR_{SUR} , with $NIR\rho_{SUR}$ in the numerator but not the denominator, was more sensitive than $NDVI_{SUR}$ to increasing LAI. An LAI increase from 2 to 4 resulted in a doubling of the SR_{SUR} compared to a 15% increase in the $NDVI_{SUR}$. However, this greater sensitivity also introduced more noise in the moderate to high LAI range compared to the $NDVI_{SUR}$.

$SAVI_{SUR}$ is similarly more sensitive than the $NDVI_{SUR}$ to changes in $NIR\rho_{SUR}$. The same pattern of greater scatter is also evident but over the whole range of LAIs. In a comparison of TM-based SVIs across a broad range of locations and vegetation types, the formulations which emphasized $NIR\rho_{SUR}$ had a greater dynamic range than $NDVI_{SUR}$ and appeared to be more sensitive to canopy structural properties (Huete et al., 1997). The reduction in $SAVI_{SUR}$ in the older conifer stands in this study was greater than was the case for $NDVI_{SUR}$, also indicating its sensitivity to structure. The strong differences in the sensitivity of the SVI_{SUR} over different LAI ranges, vegetation types, and vegetation structures suggest that the optimal SVI for establishing an empirical LAI–SVI relationship may differ depending on these factors.

The Generalized LAI–SVI Relationship

The observed increase in each SVI_{SUR} with increasing LAI at low to mid LAIs (<5) is consistent with earlier observations from a variety of ecosystems and predictions from canopy reflectance models (Huemmrich and Goward, 1997; Gobron et al., 1997; Mynenei et al., 1997). Assuming that the image processing has minimized effects of differing Sun–surface–sensor geometry (Quaidari and Vermote, 1999, this issue) and that LAI estimates are accurate (see Gower et al., 1999, this issue), the observed variation around the best fit LAI– SVI_{SUR} relationships over this LAI range are most likely associated with real differences—largely independent of LAI—among the vegetation types in the optical properties of the foliage, canopy, and background. Radiometric observations and canopy radiation transfer models suggest that leaf orientation has a strong influence on R–NIR reflectance and hence on SVIs (Baret and Guyot, 1991; Bouman, 1992; Goward et al., 1994; Gobron et al., 1997). Planophile broadleaf foliage is a better reflector (per unit leaf area) of NIR and a better absorber of R than erectophile leaf types such as grasses. Hence the broadleaf-dominated stands in this study have some of the highest $NIR\rho_{SUR}$ and in many cases the SVI_{SUR} sits above the best fit LAI– SVI_{SUR} line. Spanner et al. (1994) noted higher SRs despite lower LAIs in broadleaf alder stands compared to nearby conifer stands and likewise attributed the pattern to differential NIR reflectance. The grassland

plots, with more erectophile leaf orientation, tended to have relatively low NIR reflectance for their LAI range and to sit below the best fit LAI– SVI_{SUR} lines.

The influence of background reflectance is a second factor likely to alter SVIs independent of LAI and is evident in two instances in this study. Two of the recently clearcut stands at AND sit well below the generalized LAI– $NDVI_{SUR}$ line, an effect likely related to the contribution of reflectance from the background in open patches. Both R and NIR reflectance are conspicuously high for those stands. These plots were shifted from below the best fit line in the $NDVI_{SUR}$ plot to well above the best fit line in the $SAVI_{SUR}$ plot, suggesting an over-correction. In the grasslands plots, the red reflectance was marginally higher for the unburned sites relative to the burned sites of about the same LAI. This effect has been noted elsewhere (van Leeuwen and Huete, 1996) and is associated with R reflectance from the relatively large amount of litter.

Other factors, such as differences in chlorophyll concentration per unit leaf area, differences in leaf clumping, and the relative contribution of branches to canopy reflectance, undoubtedly also introduced variability into the LAI– SVI_{SUR} relationships, but these influences could not be resolved in this preliminary study. One evident effect of the combination of factors differing among the vegetation types was a difference in the asymptote of the LAI– SVI_{SUR} relationship. The SVI_{SUR} asymptote appears to be lowest in grassland vegetation, intermediate in broadleaf vegetation, and highest in coniferous forests.

Vegetation-Type-Specific LAI–SVI Relationships

At the grassland site, there was little relationship of LAI to the SVI_{SUR} in this study. Other studies at KNZ have found moderate to strong LAI– $NDVI$ relationships using TM imagery, but with LAIs mostly below 3.0 and $NDVIs$ generally less than those observed here (Friedl et al., 1994; Goetz, 1997). The LAIs in this study were all above 2.4, which may be near the $NDVI$ asymptote for grassland vegetation using TM imagery. Strong linear relationships and relatively high LAI– SVI asymptotes in grasslands and agricultural lands have been reported under well-controlled conditions with hand-held or boom-mounted sensors (Asrar et al., 1984; Middleton, 1991), the larger pixel size in TM imagery and possible atmospheric influences not completely removed by the image processing may constrain the operational LAI– SVI_{SUR} asymptote to a lower level.

In broadleaf stands, $NDVI_{SUR}$ was virtually unchanging across the range of LAIs. Because of the variation in NIR reflectance, there were increases in SR_{SUR} and $SAVI_{SUR}$ with increasing LAI. An earlier study in boreal aspen stands showed modest sensitivity in the response of SR_{SUR} to LAI over a lower LAI range (Badhwar et al., 1986). Thus, there appears to be reasonable prospects

for retrieval of LAI from broadleaf stands over much of their LAI range using TM imagery, although most likely not with NDVI at the highest LAIs.

For young conifer stands, $\text{NIR}\rho_{\text{SUR}}$ increased as LAI increased over the whole range from 1.5 to 9. SAVI_{SUR} with its greater sensitivity to NIR than R reflectance correspondingly increased consistently while the responses of NDVI_{SUR} and SR_{SUR} were more variable. Earlier TM-based studies in conifer stands have also reported sensitivity in SVIs at low, midrange, and high LAIs (Spanner et al., 1990; 1994; Curran et al., 1992; Nemani et al., 1993; Chen and Cihlar, 1996; Franklin et al., 1997). In low LAI stands with relatively open canopies there may be problems with reflectance from the soil or understory (Nemani et al., 1993) and in high LAI stands the relationships are asymptotic. Nevertheless, the tendency for a higher LAI asymptote in NIR reflectance for young conifer canopies than for other vegetation types means that LAI–SVI relationships may be useful for a relatively large proportion of the LAI range for this vegetation class.

For the older conifer stands with the highest LAIs, the decrease in SVI_{SUR} is driven by a reduction in NIR reflectance. The complex canopy structure in these stands (Spies and Franklin, 1991) promotes shadowing (Spanner et al., 1990; Ripple et al., 1991) and hence reduction in the NIR reflectance (Lebron et al., 1996). An appreciable decrease in SVI_{SUR} at the maximum LAIs does not appear to have been observed in tropical or broadleaf forests and is apparently not manifest in young conifer plantations (Spanner et al., 1990; Curran et al., 1992). The rounder canopy tops of broadleaf and tropical forest trees may result in fewer shadows and a more homogeneous surface at the top of the canopy.

Comparison of patterns in LAI–SVI relationships based on observations and those predicted by inversion of canopy radiation transfer models will potentially be useful in parametrization and validation of the radiation transfer models. The LAI–NDVI relationships in Myneni et al. (1997) indicate a similar dynamic range for NDVI over the range of LAIs in this study, and, in both observed and modeled cases, broadleaf forests tend to have higher NDVIs than conifer forests of the same LAI. However, the radiation transfer model indicates grasslands above LAI 3 would have a higher NDVI than broadleaf or conifer forests of a similar LAI—a relationship not observed in this study. The desirability of making such comparisons over the complete range of LAIs within a vegetation type emphasizes the need for aggregating the observational data from multiple sites into a common relationship.

Operational Mapping and Monitoring of LAI at the Landscape Scale

Validation of MODLAND LAI surfaces will require periodic comparisons to locally mapped LAI at selected sites

representative of the major global vegetation and land use types (Running et al., 1999, this issue). The nominal 1.0 km resolution of the MODLAND LAI product is much larger than the plot size typically used in LAI measurements. Thus a procedure will be needed to match the scale of the LAI measurements to the scale of the MODLAND grid cells. Extension of that procedure to produce landscape scale (10–100 km²) LAI surfaces would permit the overlay of MODLAND-generated and locally generated LAI surfaces and assessment of differences.

Although a comprehensive, physically based, scheme for assessing potential errors associated with empirical LAI–SVI relationships is just beginning to emerge (Freidl, 1997), enough work has been done across a variety of vegetation types to suggest these relationships could contribute significantly to creation of relevant validation surfaces. Imagery from TM or Enhanced Thematic Mapper+ could be used for land cover classification into broad physiognomic types (Thomlinson, 1999, this issue), and extensive ground-based LAI measurements during an interval closely associated with the imagery could be used for development of empirical, vegetation type-specific, LAI–SVI algorithms. Stratification by terrain variables may also be desirable (Friedl et al., 1994). Withholding a portion of the LAI measurements from algorithm development would permit assessment of LAI estimation error (e.g., Curran et al., 1992).

Sensors with higher spatial and/or spectral resolution than TM, or with off-nadir view angles, could potentially result in the more accurate LAI surfaces under some conditions (Curran and Williamson, 1987; Spanner et al., 1994; Peterson, 1997). However, the constraints on their coverage may not be consistent with development of a common protocol across many validation sites. A sensor with higher spatial resolution than TM may not be desirable in any case, at least in forests, because it would begin to resolve canopies of individual trees (Cohen et al., 1990) and potentially introduce heterogeneity at a finer spatial scale than that at which LAI is measured. The benefits of higher spectral resolution and off-nadir view angles for LAI estimation remain significant research issues (Johnson et al., 1994; Spanner et al., 1994).

Since some of the variability in the LAI–SVI relationships is introduced simply by uncertainty in the LAI measurements (Curran and Williamson, 1985; White et al., 1997; Gower et al., 1999, this issue), one of the early requirements in the development of an operational LAI mapping procedure based on SVIs should be a comprehensive data set of georeferenced points where LAI has been measured in a standardized manner in association with acquisition of TM imagery. Destructive sampling is arguably the most reliable LAI measurement approach, but optical approaches will be necessary to feasibly sample areas on the order of 100 km² as will be needed in the EOS validation effort (Running, 1999, this issue). Extensive research on transmittance-based LAI estimates in for-

ests (Chason et al., 1991; Fassnacht et al., 1994; Gower et al., 1999, this issue) and transmittance- or reflectance-based approaches in grasslands (Asrar et al., 1984) indicate these methods are effective but require careful calibration. Thus, an early research objective in the validation program should emphasize methods comparison studies so that the optical methods may be reliably applied in development and testing of the LAI–SVI algorithms.

Given reliable LAI measurements, one of the most obvious constraints on operational application of LAI–SVI relationships is the low sensitivity of the SVIs at high LAIs. Forests, typically with LAIs greater than 3–5, occupy approximately one third of the terrestrial land surface (Schlesinger, 1996), and validating global LAI surfaces would be most meaningful if the validation site mapping algorithms showed sensitivity to midrange LAIs. Classification into plant physiognomic types with differing foliar optical properties will help by reducing scatter in the LAI–SVI relationships. The power of TM-based classification to resolve stages of forest succession (e.g., young vs. old stands at AND; Cohen et al., 1995) could also reduce scatter associated with variation in stand structure. Nevertheless, observations and canopy reflectance models (Gobron et al., 1997; Knyazikhin et al., 1999) confirm that there will remain significant constraints on retrieving LAI with reflectance-based satellite imagery in some environments.

CONCLUSIONS

- Local mapping of LAI for a variety of sites differing in vegetation physiognomy and land use is required for the purposes of validating MODLAND LAI products.
- Empirical LAI–SVI relationships using satellite-borne sensors such as TM offer an opportunity for producing such LAI surfaces.
- Since the level of image processing significantly affects SVIs, care must be taken to account for this factor in comparing LAI–SVI studies across sites.
- Atmospherically corrected reflectance produces a stronger cross-site LAI–NDVI relationship than NDVIs based on DN, radiance, or top of atmosphere reflectance. Thus atmospheric correction is desirable in the formulation of LAI–SVI algorithms based on data from multiple sites.
- Empirical topographic corrections at the mountainous site in this study differentially affected the SVIs but did not strengthen the LAI–SVI relationships.
- Across vegetation types, the SVIs increase with LAI at low LAIs and tended to be asymptotic for LAIs greater than 5.
- In old conifer stands, SVIs declined despite high LAIs because of decreased NIR reflectance associated with gaps in the canopy which are shaded at the time of image acquisition.

- The influence of differences in the optical properties of vegetation were evident in this cross-site study and suggest the need for specificity with regard to vegetation type in the development and application of LAI–SVI relationships.
- The SVIs differ in the degree to which they respond to LAI over particular vegetation types and LAI ranges.

Support for this study was provided by the NASA Terrestrial Ecology Program (MODLERS). H. J. Andrews, North Temperate Lakes, and Konza Prairie are Long Term Ecological Research Network sites and are supported through grants from the National Science Foundation.

REFERENCES

- Asrar, G., Fuchs, M., Kanemasu, E. T., and Hatfield, J. L. (1984), Estimating absorbed photosynthetic radiation and leaf area index from spectral reflectance in wheat. *Agron. J.* 76:300–306.
- Badhwar, G. D., MacDonald, R. B., Hall, F. G., and Carnes, J. G. (1986). Spectral characterization of biophysical characteristics in a boreal forest: relationship between Thematic Mapper band reflectance and leaf area index for aspen. *IEEE Trans. Geosci. Remote Sens.* GE-24:322–326.
- Baret, F., and Guyot, G. (1991), Potentials and limits of vegetation indices for LAI and APAR assessment. *Remote Sens. Environ.* 35:161–173.
- Barnes, B. V., and Wagner, W. H. (1981), *Michigan Trees: a Guide to Trees of Michigan and the Great Lakes Region*. University of Michigan Press, Ann Arbor.
- Bonan, G. B. (1995). Land–atmosphere interactions for climate system models: coupling biophysical, biogeochemical, and ecosystem dynamical processes. *Remote Sens. Environ.* 51: 57–73.
- Bouman, B. A. (1992), Accuracy of estimating the leaf area index from vegetation indices derived from crop reflectance characteristics, a simulation study. *Int. J. Remote Sens.* 13: 3069–3084.
- Briggs, J. M., and Knapp, A. K. (1995), Interannual variability in primary production in tallgrass prairie: climate, soil moisture, topographic position and fire as determinants of above-ground biomass. *Am. J. Bot.* 82:1024–1030.
- Burton, A. J., Pregetzer, K. S., and Reed, D. R. (1991), Leaf area and foliar biomass relationships in northern hardwood forests located along an 800 km acid deposition gradient. *For. Sci.* 37:1041–1059.
- Cannell, M. G. (1982), *World Forest Biomass and Primary Production Data*, Academic Press, London.
- Chase, T. N., Pielke, R. A., Kittel, T. G. F., Running, S. R., and Nemani, R. (1996), Sensitivity of a general circulation model to global changes in leaf area index. *J. Geophys. Res.* 101:7393–7408.
- Chason, J. W., Baldocchi, D. D., and Huston, M. A. (1991). A comparison of direct and indirect methods for estimating forest canopy leaf area. *Agri. For. Meteorol.* 57:107–128.
- Chen, J. M. (1996), Evaluation of vegetation indices and a

- modified simple ratio for Boreal applications. *Can. J. Remote Sens.* 22:229–242.
- Chen, J. M., and Cihlar, J. (1996), Retrieving leaf area index of boreal conifer forests using Landsat TM images. *Remote Sens. Environ.* 55:153–162.
- Cohen, W. B., and Spies, T. A. (1992), Estimating structural attributes of Douglas-fir/western hemlock forest stands from Landsat and SPOT imagery. *Remote Sens. Environ.* 41:1–17.
- Cohen, W. B., Spies, T. A., and Bradshaw, G. A. (1990), Semi-variograms of digital imagery for analysis of conifer canopy structure. *Remote Sens. Environ.* 34:167–178.
- Cohen, W. B., Spies, T. A., and Fiorella, M. (1995), Estimating the age and structure of forests in a multi-ownership landscape of western Oregon, U.S.A. *Int. J. Remote Sens.* 16:721–746.
- Curran, P. J., and Williamson, H. D. (1985), The accuracy of ground data used in remote sensing investigations. *Int. J. Remote Sens.* 6:1637–1651.
- Curran, P. J., and Williamson, H. D. (1987), Estimating the green leaf area index of grassland with airborne multispectral scanner data. *Oikos* 49:141–148.
- Curran, P. J., Dungan, J. L., and Gholz, H. L. (1992), Seasonal LAI in slash pine estimated with Landsat TM. *Remote Sens. Environ.* 39:3–13.
- Deering, D. W., Middleton, E. M., and Eck, T. F. (1994), Reflectance anisotropy for a spruce-hemlock forest canopy. *Remote Sens. Environ.* 47:242–260.
- Epiphanio, J. C. N., and Huete, A. R. (1995), Dependence of NDVI and SAVI on sun/sensor geometry and its effect on f_{APAR} relationships in alfalfa. *Remote Sens. Environ.* 51:351–360.
- Fassnacht, K. S., Gower, S. T., Norman, J. M., and McMurtrie, R. E. (1994), A comparison of optical and direct methods for estimating foliage surface area index in forests. *Agri. For. Meteorol.* 71:183–207.
- Fassnacht, K. S., Gower, S. T., MacKenzie, M. D., Nordheim, E. V., and Lillesand, T. M. (1997), Estimating the leaf area index of north central Wisconsin forests using the Landsat Thematic Mapper. *Remote Sens. Environ.* 61:229–245.
- Franklin, J. (1986), Thematic Mapper analysis of coniferous forest structure and composition. *Int. J. Remote Sens.* 10:1287–1301.
- Franklin, S. E., Lavigne, M. B., Deuling, M. J., Wulders, M. A. and Hunt, E. R. (1997), Estimation of forest Leaf Area Index using remote sensing and GIS data for modelling net primary production. *Int. J. Remote Sens.* 18:3459–3471.
- Friedl, M. A. (1997), Examining the effects of sensor resolution and sub-pixel heterogeneity on spectral vegetation indices: implications for biophysical modeling. In *Scale in Remote Sensing* (D. A. Quattrochi and M. F. Goodchild, Eds.), Lewis Publishers, Boca Raton, FL, pp 113–139.
- Friedl, M. A., Michaelsen, J., Davis, F. W., Walker, H., and Schimel, D. S. (1994), Estimating grassland biomass and leaf area index using ground and satellite data. *Int. J. Remote Sens.* 15:1401–1420.
- Gates, D., Keegan, J. J., Schleter, J. C., and Weidner, V. R. (1965), Spectral properties of plants. *Appl. Opt.* 4:11–20.
- Gobron, N., Pinty, B., and Verstraete, M. M. (1997), Theoretical limits to the estimation of the leaf area index on the basis of visible and near-infrared remote sensing data. *ISEE Trans. Geosci. Remote Sens.* 35:1438–1445.
- Goetz, S. J. (1997), Multi-sensor analysis of NDVI, surface temperature and biophysical variables at a mixed grassland site. *Int. J. Remote Sens.* 18:71–94.
- Goward, S. N., Markham, B., Dye, D. G., Dulaney, W., and Yang, J. (1991), Normalized difference vegetation index measurements from the Advanced Very High Resolution Radiometer. *Remote Sens. Environ.* 35:257–277.
- Goward, S. N., Huemmrich, K. F., and Waring, R. H. (1994), Visible-near-infrared spectral reflectance of landscape components in western Oregon. *Remote Sens. Environ.* 47:190–203.
- Gower, S. T., Kucharik, C. J., and Norman, J. M. (1999), Direct and indirect estimation of leaf area index, f_{APAR} , and net primary production of terrestrial ecosystems. *Remote Sens. Environ.* 70:29–51.
- Guyot, G., Guyon, D., and Riou, J. (1989), Factors affecting the spectral response of forest canopies: a review. *Geocarta Int.* 4:3–18.
- Hall, F. G., Townshend, J. R., and Engman, E. T. (1995), Status of remote sensing algorithms for estimation of land surface state parameters. *Remote Sens. Environ.* 51:138–156.
- Hansen, A. J., Garman, S. L., Marks, B., and Urban, D. L. (1993), An approach for managing vertebrate diversity across multiple landscapes. *Ecol. Appl.* 3:481–496.
- Huemmrich, K. F., and Goward, S. N. (1997), Vegetation canopy PAR absorbance and NDVI: an assessment for ten tree species with the SAIL model. *Remote Sens. Environ.* 61:254–269.
- Huete, A. R. (1988), A soil-adjusted vegetation index (SAVI). *Remote Sens. Environ.* 25:295–309.
- Huete, A. R., and Tucker, C. J. (1991), Investigation of soil influences in AVHRR red and near-IR vegetation index imagery. *Int. J. Remote Sens.* 12:1223–1242.
- Huete, A., Justice, C., and Liu, H. (1994), Development of vegetation and soil indices for MODIS-EOS. *Remote Sens. Environ.* 49:224–234.
- Huete, A. R., Liu, H. Q., Batchily, K., and van Leeuwen, W. (1997), A comparison of vegetation indices over a global set of TM Images for EOS-MODIS. *Remote Sens. Environ.* 59:440–451.
- Hunt, E. R., Jr., Piper, S. C., Nemani, R., Keeling, C. D., Otto, R. D., and Running, S. W. (1996), Global net carbon exchange and intra-annual atmospheric CO₂ concentrations predicted by an ecosystem process model and three-dimensional atmospheric transport model. *Global Biogeochem. Cycles* 10:431–456.
- Jackson, R. D. (1983), Spectral indices in n -spaces. *Remote Sens. Environ.* 13:409–421.
- Johnson, L. F., Hlavka, C. A., and Peterson, D. L. (1994), Multivariate analysis of AVIRIS data for canopy biochemical estimation along the Oregon transect. *Remote Sens. Environ.* 47:216–230.
- Jordan, C. F. (1969), Deviation of leaf-area index from quality of light on the forest floor. *Ecology* 50:663–666.
- Justice, C. O., Eck, T. F., Tanre, D., and Holben, B. N. (1991), The effect of water vapor on the normalized difference vegetation index derived for the Sahelian region from NOAA AVHRR data. *Int. J. Remote Sens.* 12:1165–1187.
- Knyazikhin, Y., Martonchik, J. V., Myneni, R. B., Diner, D. J., and Running, S. W. (1999), Synergistic algorithm for estimating vegetation canopy leaf area index and fraction of ab-

- sorbed photosynthetically active radiation from MODIS and MISR data. *J. Geophys. Res.*, in press.
- Law, B. E., and Waring, R. H. (1994), Remote sensing of leaf area index and radiation intercepted by understory vegetation. *Ecol. Appl.* 4:272–279.
- Leblon, B., Gallant, L., and Grandberg, H. (1996), Effects of shadowing types on ground-measured visible and near-infrared shadow reflectances. *Remote Sens. Environ.* 58:322–328.
- Markham, B. L., and Barker, J. L. (1986), Landsat MSS and TM post-calibration dynamic ranges, exoatmospheric reflectances and at-satellite temperatures, EOSTAT Landsat Technical Notes, No. 1, NASA, Greenbelt, MD, pp. 3–8.
- Martin, M. E., and Aber, J. D. (1997), Estimating forest canopy characteristics as inputs for models of forest carbon exchange by high spectral resolution remote sensing. In *The Use of Remote Sensing in the Modeling of Forest Productivity* (H. L. Gholz, K. Nakane, and H. Shimoda, Eds.), Kluwer Academic, London, pp. 61–72.
- Means, J. E., Hansen, A. H., Koerper, G. J., Alaback, P. B., and Klopsch, M. W. (1994), Software for computing plant biomass–BIOPAK users guide, Gen. Tech. Rep. PNW-GTR-340, USDA Forest Service, Pacific Northwest Research Station, Portland, OR, 184 pp.
- Means, J. E., Acker, S. A., Harding, D. A., et al. (1999), Use of large-footprint scanning airborne lidar to estimate forest stand characteristics in the western Cascades of Oregon. *Remote Sens. Environ.* 67:298–308.
- Middleton, E. M. (1991), Solar zenith angle effects on vegetation indices in tallgrass prairie. *Remote Sens. Environ.* 38:45–62.
- Meyer, P., Itten, K. I., Kellenberger, T., Sandmeirer, S., and Sandmeirer, R. (1993), Radiometric corrections of topographically induced effects on Landsat TM data in an alpine environment. *Photogramm. Eng. Remote Sens.* 48:17–28.
- Milner, K. S., Running, S. W., and Coble, D. W. (1996), A biophysical soil-site model for estimating potential productivity of forested landscapes. *Can. J. For. Res.* 26:1174–1186.
- Myneni, R. B., and Asrar, G. (1994), Atmospheric effects and spectral vegetation indices. *Remote Sens. Environ.* 47:390–402.
- Myneni, R. B., Maggion, S., Jaquinta, J., et al. (1995), Optical remote sensing of vegetation: modeling, caveats, and algorithms. *Remote Sens. Environ.* 51:169–188.
- Myneni, R. B., Nemani, R. R., and Running, S. W. (1997), Estimation of global leaf area index and absorbed PAR using radiative transfer models. *IEEE Geosci. Remote Sens.* 35:1380–1393.
- Nemani, R. R., Pierce, L., Running, S. W., and Band, L. (1993), Forest ecosystem processes at the watershed scale: Sensitivity to remotely-sensed leaf area index estimates. *Int. J. Remote Sens.* 14:2519–2534.
- Peterson, D. L. (1997), Forest structure and productivity along the Oregon transect. In *The Use of Remote Sensing in the Modeling of Forest Productivity* (H. L. Gholz, K. Nakane, and H. Shimoda, Eds.), Kluwer Academic, London, pp. 173–217.
- Peterson, D. L., Spanner, M. A., Running, S. W., and Teuber, K. B. (1987), Relationship of thematic mapper simulator data to leaf area index of temperate coniferous forests. *Remote Sens. Environ.* 22:323–341.
- Price, J. C., and Bausch, C. (1995), Leaf area index estimation from visible and near-infrared reflectance data. *Remote Sens. Environ.* 52:55–65.
- Ouaidrari, H., and Vermote, E. F. (1999), Operational atmospheric correction of Landsat TM data. *Remote Sens. Environ.* 70:4–15.
- Richardson, A. J., and Wiegand, C. L. (1977), Distinguishing vegetation from soil background information. *Photogramm. Eng. Remote Sens.* 43:1541–1552.
- Ripple, W. J., Wang, S., Isaacson, D. L., and Paine, D. P. (1991), A preliminary comparison of Landsat Thematic Mapper and SPOT-1 HRV multispectral data for estimating coniferous forest volume. *Int. J. Remote Sens.* 12:1971–1977.
- Running, S. W. (1990), A bottom-up evolution of terrestrial ecosystem modeling theory, and ideas toward global vegetation modeling. In *Modeling the Earth System* (D. Ojima, Ed.), UCAR/Office for Interdisciplinary Earth Studies, Boulder, CO, pp. 263–280.
- Running, S. W., Peterson, D. L., Spanner, M. A., and Teuber, K. B. (1986), Remote sensing of coniferous forest leaf area. *Ecology* 67:273–276.
- Running, S. W., Nemani, R. R., Peterson, D. L., et al. (1989), Mapping regional forest evapotranspiration and photosynthesis by coupling satellite data with ecosystem simulation. *Ecology* 70:1090–1101.
- Running, S. W., Justice, C. O., Salmonson, V., et al. (1994), Terrestrial remote sensing science and algorithms planned for EOS/MODIS. *Int. J. Remote Sens.* 15:3587–3620.
- Running, S. W., Baldocchi, D., Turner, D. P., Gower, S. T., Bakwin, P. S., and Hibbard, K. A. (1999), A global terrestrial monitoring network integrating tower fluxes, flask sampling, ecosystem modeling and EOS satellite data. *Remote Sens. Environ.* 70:108–127.
- SAS Institute, Inc. (1990), *SAS/STAT User's Guide, Version 6*, 4th ed., SAS Institute, Inc. Cary, NC, Vols. 1–2.
- Schlesinger, W. H. (1996), *Biogeochemistry*, Academic, San Diego, CA, 443 pp.
- Spanner, M. A., Pierce, L. L., Peterson, D. L., and Running, S. W. (1990), Remote sensing of temperate coniferous forest leaf area index: the influence of canopy closure, understory vegetation and background reflectance. *Int. J. Remote Sens.* 11:95–111.
- Spanner, M. A., Johnson, L., Miller, J., et al. (1994), Remote sensing of seasonal leaf area index across the Oregon transect. *Ecol. Appl.* 4:258–271.
- Spies, T. A., and Franklin, J. F. (1991), The structure of natural young, mature, and old-growth Douglas-fir forests in Oregon and Washington. In *Wildlife and Vegetation in Unmanaged Douglas-Fir Forests* (L. F. Ruggiero, K. B. Aubry, A. B. Carey, and M. H. Huff, technical coordinators), General Technical Report PNW-6TR-285, USDA Forest Service, Pacific Northwest Research Station, Portland, OR, pp. 91–109.
- Su, H., Briggs, J. M., Knapp, A. K., Blair, J. M., and Krummel, J. R. (1996), Detecting spatial and temporal patterns of aboveground production in a tallgrass prairie using remotely sensed data. *IEEE Trans. Geosci. Remote Sens.* 4:2361–2365.
- Thomlinson, J. R., Bolstad, P. V., and Cohen, W. B. (1999), Coordinating methodologies for scaling landcover classifications from site-specific to global: steps toward validating global map products. *Remote Sens. Environ.* 70:16–28.
- Tiellet, P. M., Staenz, K., and Williams, D. J. (1997), Effects of

- spectral, spatial, and radiometric characteristics on remote sensing vegetation indices of forested regions. *Remote Sens. Environ.* 61:139–149.
- Tucker, C. J. (1979), Red and photographic infrared linear combinations for monitoring vegetation. *Remote Sens. Environ.* 8:127–150.
- Turner, D. P., Acker, S. A., Means, J. E., and Garman, S. L. (1999), Assessing alternative allometric algorithms for estimating leaf area index in Douglas-fir trees and stands. *For. Ecol. Manage.*, in press.
- Urban, D. L. (1993), A user's guide to ZELIG version 2, Department of Forest Sciences, Colorado State University, Ft. Collins, 77 pp.
- Urban, D. L., Harmon, M. E., and Halpern, C. B. (1993), Potential response of Pacific Northwestern forests to climatic change, effects of stand age and initial composition. *Clim. Change* 23:247–266.
- Van Cleve, K., and Martin, S. (1991), *Long-Term Ecological Research in the United States*, LTER Research Network Office, University of Washington, Seattle.
- van Leeuwen, W. J. D., and Huete, A. R. (1996), Effects of standing litter on the biophysical interpretation of plant canopies with spectral indices. *Remote Sens. Environ.* 55:123–138.
- Waring, R. H., Gholz, H. L., Grier, C. C., and Plummer, M. L. (1977), Evaluating stem conducting tissue as an estimator of leaf area in four woody angiosperms. *Can. J. Bot.* 55:1474–1477.
- White, J. D., Running, S. W., Nemani, R., Keane, R. E., and Ryan, K. C. (1997), Measurement and remote sensing of LAI in Rocky Mountain montane ecosystems. *Can. J. For. Res.* 27:1714–1727.
- Wiegand, C. L., Richardson, A. J., and Kanemasu, E. T. (1979), Leaf area index estimates for wheat from LANDSAT and their implications for evapotranspiration and crop modeling. *Agron. J.* 71:336–342.
- Williams, D. L. (1991), A comparison of spectral reflectance properties at the needle, branch, and canopy level for selected conifer species. *Remote Sens. Environ.* 35:79–93.
- Yoder, B. J., and Waring, R. H. (1994), The normalized difference vegetation index of small Douglas-fir canopies with varying chlorophyll concentrations. *Remote Sens. Environ.* 49:81–91.